Computational Materials Science

The influence of crack on the Si anode performance in Na- and Mg-ion batteries: An atomic multiscale study

--Manuscript Draft--

Manuscript Number:	COMMAT-D-21-03078
Article Type:	Full Length Article
Section/Category:	Atomic Description
Keywords:	Na-ion battery; Mg-ion battery; Si anode; multiscale simulation; crack
Abstract:	Based on multiscale simulations coupled with quantum mechanical and molecular mechanical methods, we present the impact of crack on the performance of Si anode in Na-ion batteries (NIBs) and Mg-ion batteries (MIBs). We found that crack can offer more stable sites to host interstitials than defect-free Si and form binding energy gradients near the crack front. Moreover, the crack tip may significantly enhance the binding strength, enabling it to insert Na and Mg into the Si anode thermodynamically. The crack creates a fast channel into the tip along its propagation direction, causing Na and Mg to accumulate at the crack tip, similar to the case of Li. Furthermore, since diffusion out is more challenging, Na and Mg prefer to diffuse into the crack. Finally, the crack may also trap interstitials and lower the charging and discharging rate of NIBs and MIBs.

The influence of crack on the Si anode performance in Na- and Mg-ion batteries: An atomic multiscale study

Chaoying Wang[1], Chao Zhang[1], Qianli Xue[1],Chenliang Li[1], Baolai Wang[1,*], Lijun Yang[2] and Zailin Yang[1,*]

[1]*College of Aerospace and Civil Engineering, Harbin Engineering University, Harbin 150001, People's Republic of China*

[2]*Key Laboratory of Mesoscopic Chemistry of MOE, School of Chemistry and Chemical Engineering, Nanjing University, Nanjing 210093, People's Republic of China*

Based on multiscale simulations coupled with quantum mechanical and molecular mechanical methods, we present the impact of crack on the performance of Si anode in Na-ion batteries (NIBs) and Mg-ion batteries (MIBs). We found that crack can offer more stable sites to host interstitials than defect-free Si and form binding energy gradients near the crack front. Moreover, the crack tip may significantly enhance the binding strength, enabling it to insert Na and Mg into the Si anode thermodynamically. The crack creates a fast channel into the tip along its propagation direction, causing Na and Mg to accumulate at the crack tip, similar to the case of Li. Furthermore, since diffusion out is more challenging, Na and Mg prefer to diffuse into the crack. Finally, the crack may also trap interstitials and lower the charging and discharging rate of NIBs and MIBs.

KEYWORDS: Na-ion battery, Mg-ion battery, Si anode, multiscale simulation, crack

1. Introduction

Rechargeable metal-ion batteries are attracting interest for their convenience and wide applications in energy storage [1-3]. Particularly, Li-ion batteries (LIBs) are

* Corresponding authors.
E-mail addresses:wangbaolai1979@sina.com (B. Wang), yangzailinheu@163.com (Z. Yang)

widely studied and used commercially [4-6]. However, with increasing global demands, the conflict between limited lithium resources and the expansion of applications could become more acute [7]. Therefore, new batteries made of abundant and cheap metal materials need to be developed to replace LIBs. Na and Mg are popularly seen as alternatives to Li as they have a relatively low price and similar alloying chemistry [2,3,8-10]. The critical issue with the commercialization of Na-ion batteries (NIBs) and Mg-ion batteries (MIBs) is finding high-performance anode materials. As a negative electrode material, Si offers relatively high theoretical Li, Na, and Mg capacities of about 4200, 950, and 3280 mAh/g, respectively [11]. Several studies have investigated the interactions of Na [12-17] and Mg [13,16-18] with defect-free Si. The ionic radii of Na and Mg are larger than that of Li, making them more challenging to embed in crystalline silicon (c-Si). Since the binding energies of Na and Mg are negative in perfect c-Si, both the insertions are thermodynamically unfavored [17-20]. Previous density functional theory (DFT) calculations indicate that Al doping can significantly improve Na and Mg's binding energies [16]. Moreover, dislocations in Si anode could promote the binding energies to positive values by providing ample spaces to accommodate Na and Mg [17,21]. However, very little attention has been paid to the role of crack, which has been widely investigated in the study of Si anode for LIBs [22-24].

During the insertion, metal atoms may react with Si to form M_xSi (M=Li, Na, and Mg) alloy [18,25,26], followed by a considerable volume expansion [18,25-28]. For LIBs, the volume change experienced by the Si negative electrode is up to 400% [28]. Consequently, there are mismatch stresses at the junction of expanded and unexpanded regions [11,29-31]. Moreover, lithiation-induced stresses may cause Si anode cracking [22-24]. Many experiments illustrated that these cracks might

propagate deep into the c-Si [32-34] and become highways for Li insertion [34]. In recent experiments, molecular dynamics (MD) simulations and fully coupled finite element analyses have shown that Li may concentrate at the crack tip [35-36]. The volume changes for NaSi and Mg_2Si formations are 144% [26] and 216% [16], respectively. With increased interstitial concentration, cracks may also initiate and propagate in the Si anode to release the mismatch stress. Crack provides more space to host metal atoms [36] and may make the Si anode suitable for Na and Mg storage. However, the effect of cracks on the distribution and diffusion of Na and Mg is still unknown.

This work reports a multiscale simulation study on the influence of cracks on the storage, charge and discharge rate of NIBs and MIBs at the atomic level. This study investigates Na and Mg's energy-favorite sites and binding energies within and around the crack front, their diffusion, and the corresponding barriers.

2. Methodology

Sufficient model size is required in MD simulations to characterize the long-range strain field and structural features of the crack at the expense of reduced computational efficiency and accuracy in dynamic calculations. Besides, the interactions between guest atoms and the host require the DFT, which has strict limitations on the model size. The current work employs the multiscale approach of coupling quantum mechanics (QM) and molecular mechanics (MM) [37] to characterize both the stress concentration of crack tip and the chemical properties of Na and Mg [38,39]. The entire model comprises two main regions: MM and QM parts. The left crack tip and the surrounding area (represented as balls in Fig. 1a) were selected as the QM zone and processed using the DFT (SIESTA code) [40]. The remainder, i.e., the MM part, was processed using the Large-scale Atomic/Molecular

Massively Parallel Simulator (LAMMPS) software package [41] with the charge-optimized many-body functional potential (COMB) [42]. The multiscale simulation was performed by continuously alternating MD and DFT calculations to achieve a maximum force in the QM region smaller than 0.001 eV/Å. The interaction forces between the two parts are exchanged by the outermost layer atoms of the QM region (gray balls in Fig. 1a) to eliminate the mismatch.

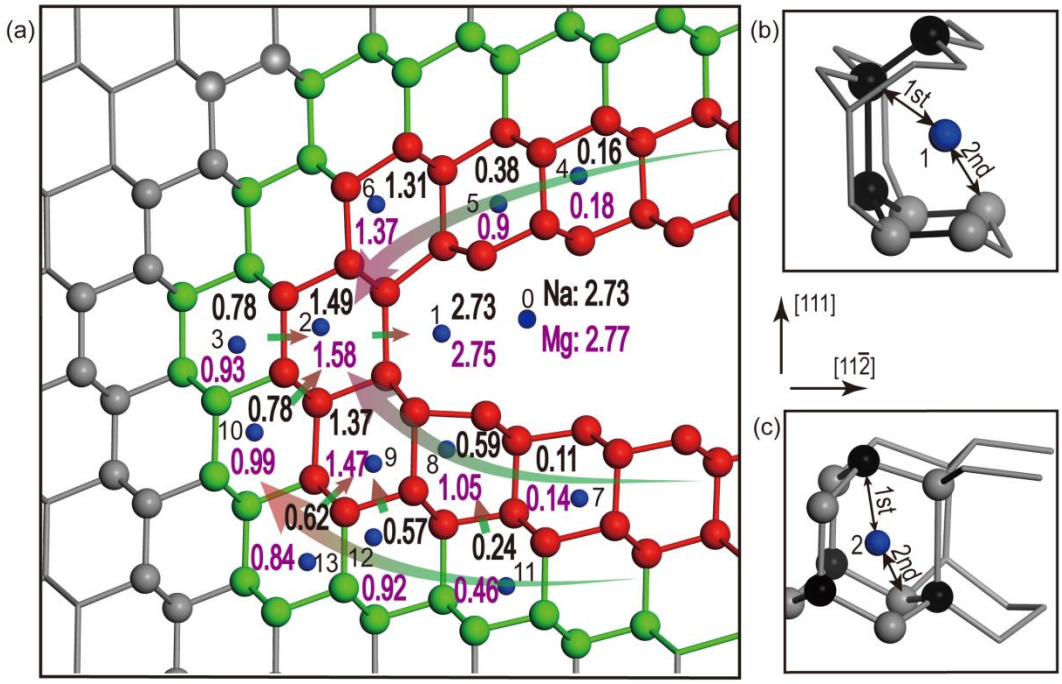

Fig. 1. (a) The energy favorite sites and corresponding binding energy differences (eV) of Na (black number) and Mg (red number) in front of the crack with respect to perfect c-Si. (b-c) The first nearest neighbors (black balls) and the second nearest neighbors (gray balls) of Na and Mg at sites 1 and 2.

A pre-cracked model was prepared with dimensions of 159.7×341.8×15.2 Å in the [111], [11$\bar{2}$] and [1$\bar{1}$0] directions, respectively. The crack propagation direction is [11$\bar{2}$] with the lowest energy (111) crack surface [38,43]. The MD method applied the mode I loading on the initial crack in the [111] direction. When the crack was about to propagate critically, the upper and lower boundaries were fixed to optimize the model

structure. The crack's left region containing 400 atoms was selected as the QM part for DFT calculations with a 1×1×4 *k*-point sampling. The exchange-correlation functional was approximated by the generalized gradient approximation (GGA) of the Perdew–Burke–Ernzerhof (PBE) formulation [44]. An energy cutoff of 200 Ry defined the real space grid and a 100 meV energy shift was applied for a doubled-ζ polarized (DZP) basis set. Both the MD and DFT calculations involved periodic boundary conditions in three directions. More details about the validity of the multiscale simulation method and parameter settings can be found in our previous work [17,36].

The equation calculates Na and Mg's binding energies (E_b): $E_b=E_{Si}+E_M-E_{Si\text{-}M}$, where $E_{Si\text{-}M}$ and E_{Si} represent the model energies with and without M (M=Na and Mg), respectively, and E_M is the single M atom's energy estimated using the DFT. The current work focuses on determining the diffusion trajectory and energy paths using the Projected Conjugate Gradient (PCG) approach [45].

3. Results and discussion

The present work investigated Na and Mg's stable positions and binding energies in the stressed crack tip to study the potential effect of cracks on the storage of interstitials. Fig. 1a shows the hollow sites of crack surface closer to the tip (site 0), the core of the crack tip (sites 1 and 2), and its surrounding areas (site 3–13), selected to find suitable locations to store Na and Mg. Similar to the real free surface with high adsorption energy [19], the binding energies of Na (Mg) at site 0 are 1.94 eV (1.8 eV), about 2.73 eV (2.77 eV) higher than the tetrahedral (T_d) site of c-Si [17]. In the center and surrounding regions of the crack tip, site 1 is the most stable position with the highest binding energy. Table 1 and Fig. 1a indicate that the binding energies of Na

(Mg) at this location are 2.73 eV (2.75 eV) higher than the T_d site. Site 2 belongs to the uncracked side, the second stable position with the binding energy of Na (Mg) as 0.7 eV (0.61 eV). Fig. 1a shows that sites 6 and 9 can also promote the binding energies substantially, allowing the stable concentration of Na and Mg. The first and second nearest Na–Si and Mg–Si distances of sites 1 and 2, shown in Fig. 1b-c and Table 1, explain the crack's role in improving the performance of the Si negative electrode for metal atoms storage. At site 1, those Na–Si (Mg–Si) distances are 0.53 Å (0.23 Å) and 0.35 Å (0.56 Å) longer than those at the T_d site, respectively. The nearest Na–Si and Mg–Si distances of site 2 are smaller than those at site 1 and larger than those at the T_d site. Comparisons indicate that crack may provide more spaces for the compressed interstitials than c-Si and make the Na and Mg insertions energy favored.

Table 1 The binding energies E_b (eV), first (1st), and second (2nd) nearest neighbor distances (Å) of Na and Mg at site 1, site 2, and T_d.

position	E_b (Na)	Na–Si (1st)	Na–Si (2nd)	E_b (Mg)	Mg–Si (1st)	Mg–Si (2nd)
site1	1.94	3.05	3.14	1.78	2.76	3.35
site2	0.70	2.75	3.04	0.61	2.64	2.96
c-Si (T_d)	−0.79	2.52	2.79	−0.969	2.53	2.79

Fig. 1a also represents the binding energy differences of Na and Mg surrounding the front of the crack compared with the most stable T_d site of c-Si. Due to the atomic structure properties and the stress concentration of the crack tip, the binding energies of Na (Mg) are at least 0.11 eV (0.14 eV) higher than those of the c-Si. The accumulation of Na and Mg around the crack tip is thermodynamically favorable, analogous to the Li redistribution with the appearance of crack [35,36]. As shown by

the large arrows on both sides of the crack in Fig. 1a, the closer Na and Mg are to the crack tip, the greater are their binding energies. Moreover, the binding energies of the first circle (red balls) are at least 0.35 eV higher than those of the neighboring sites of the second circle (green balls). These results indicate a binding energy gradient around the front of the crack, corresponding to the stress gradient at the crack tip. Thus, we can conclude that decreasing Na and Mg's distance from the crack tip increases their thermodynamic stability, as is true for Li as well [36].

Na (Mg) moves from one T_d site to a neighboring site with an energy barrier of 1.04 eV (1.02 eV) in defect-free c-Si [17]. As cracks have modified the crystal structure and stress state in the local region, they may affect the dynamic properties of interstitials. First, Na and Mg diffusion between sites 0 and 5 is investigated for revealing how cracks influence interstitial migration in the direction perpendicular to the crack surface. As shown in Fig. 2a, Na and Mg diffuse into the crack almost along a straight line from site 5. Since this site is stable around the crack tip, the energies presented in Fig. 2b-c gradually rise to a high point until Na and Mg arrive at the interface. Simultaneously, the energy curves reach a peak when interstitials are in the center of the hexagonal ring (site T). The energy difference of 1.37 eV (1.46 eV) between sites 5 and T can be considered as the energy barrier of Na (Mg) diffusion into the crack tip area, about 0.33 eV (0.44 eV) higher than the barrier in defect-free c-Si. This is mainly because the crack provides larger spaces around the tip for Na and Mg storage, increasing the energy difference between these two sites. Moreover, increased spaces decrease energy after Na and Mg transportation into the crack (Fig. 2b-c). Finally, the energy path falls to its lowest point at site 0. The barrier of 3.72 eV (3.33 eV) between sites T and 0 is the energy to overcome for Na (Mg) to diffuse out of the crack. Since site 0 is more stable than site 5, this barrier is 2.35 eV (1.87 eV)

higher than the inverse direction. The above results show that Na and Mg migration into the crack tip is favored thermodynamically and kinetically in the direction perpendicular to the crack surface and not in the opposite direction. Considering similar atomistic structures along the crack surface, the above conclusion may also apply to other crack parts away from the tip.

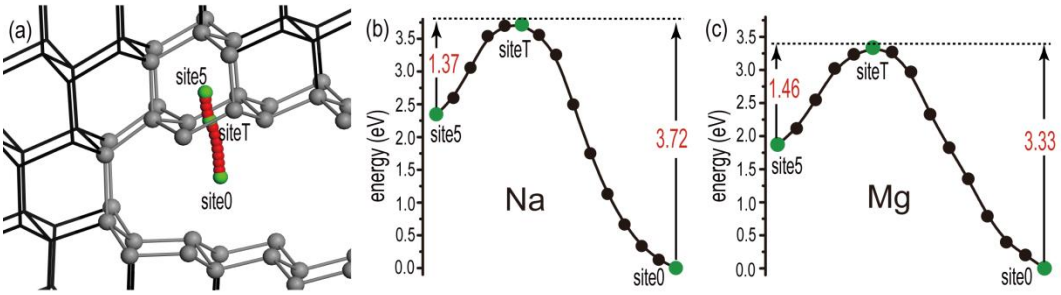

Fig 2. (a) Trajectories of Na and Mg diffusion into and outside the crack tip, and (b)-(c) the corresponding migration barriers

The diffusion of Na and Mg between the crack tip (site 1) and surrounding areas (sites 2 and 3) is investigated to determine its dynamic properties along the crack propagation direction. These sites also connect the cracked and uncracked areas on the cleavage plane. Figs. 3 and 4 show the corresponding minimum energy path and relative energy variations of Na and Mg, respectively. The energy of site 1 is considered as the reference zero energy. Na moves toward the crack tip with increasing energy from stable site 3 (Fig. 3a–c). When the interstitial is close to the center of the hexagonal channel (interface of sites 2 and 3), the available space can no longer accommodate Na with large atomic radii. Atoms 1 and 2 adjacent to the interstitial are pushed to the dashed circle positions to form the decagonal ring (Fig. 3d). Simultaneously, Na deviates from its original linear diffusion path to the location (site T_{23}) near the center of the decagonal ring. The deformation caused by two atoms being far from their stable positions results in higher level energies of the entire system during the passage of interstitial atoms in the decagonal ring. After passing

through the interface, atoms 1 and 2 (Fig. 3a) return to their original positions. The migration trajectories also switch to the original straight-line path before arriving at site 2. Once Na moves from site 2 to site 1, the Si–Si bond between atoms 3 and 4 blocks the diffusion path. Consequently, the energy curve reaches a local high point at site T. When it migrates further toward the crack tip, the path is forced to shift to the nearby trajectory. The corresponding energy should have been a peak at the center of another hexagonal channel (site T_{12}). However, the crack tip in tension provides more space and reduces the site energy.

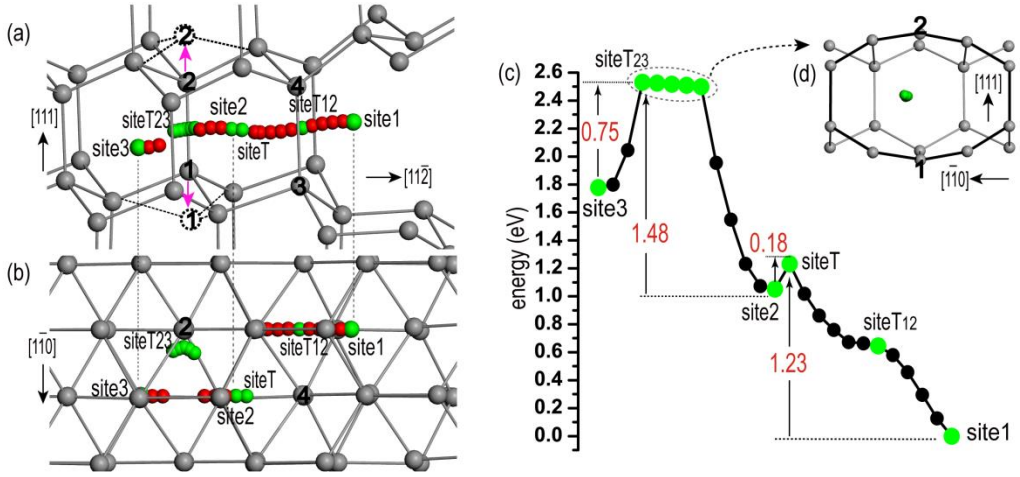

Fig. 3. (a-b) Trajectories of Na and Mg diffusion between sites 3 and 1, and (c) the corresponding migration barriers.

Fig. 3c shows that Na overcomes two barriers of 0.75 eV and 0.18 eV to diffuse from site 3 to site 1. Notably, the migration barriers decrease toward the crack tip. These two values are 0.29 eV and 0.86 eV lower than the result of Na diffusion in c-Si, respectively. Thus, the crack tip creates a rapid route for Na to diffuse into the crack in the (111) plane. Na has to conquer the barriers of 1.23 eV and 1.48 eV to diffuse out of the crack tip in the opposite direction. The migration barrier comparisons in both directions suggest that Na diffusion into the crack tip is more kinetically favorable than diffusing out. Moreover, the step-down energies of sites 3, 2, and 1 in Fig. 3c

indicate that Na diffusion into the crack tip is also thermodynamically favorable, which is consistent with these regions' binding energy gradient.

The migration of Mg toward the crack tip varies from Na's at the interface (site T_{23}). Near the center of this hexagonal channel, the corresponding energy path peaks at site T_{23}. The subsequent diffusion processes show that atom 2 (Fig. 4d) or atom 1 (Fig. 4e) deviates from its original position to form a decagonal ring allowing the passage of Mg. Unlike Na, only one atom has left its stable position, with trajectory energies lower than the maximum value. Similar to the case of Na, the barriers of Fig. 4c indicate that crack may also provide a rapid pathway for Mg to accumulate at the crack tip. Furthermore, the diffusion of both interstitials into the crack tip is kinetically and thermodynamically favorable but not in the opposite direction. Together with the binding energy results, crack tip may offer more stable and easy in but hard out sites to store Na and Mg. Thus, interstitials may be trapped in the crack and the charging/discharging capacity of NIBs and MIBs may be weakened, similar to LIBs [36].

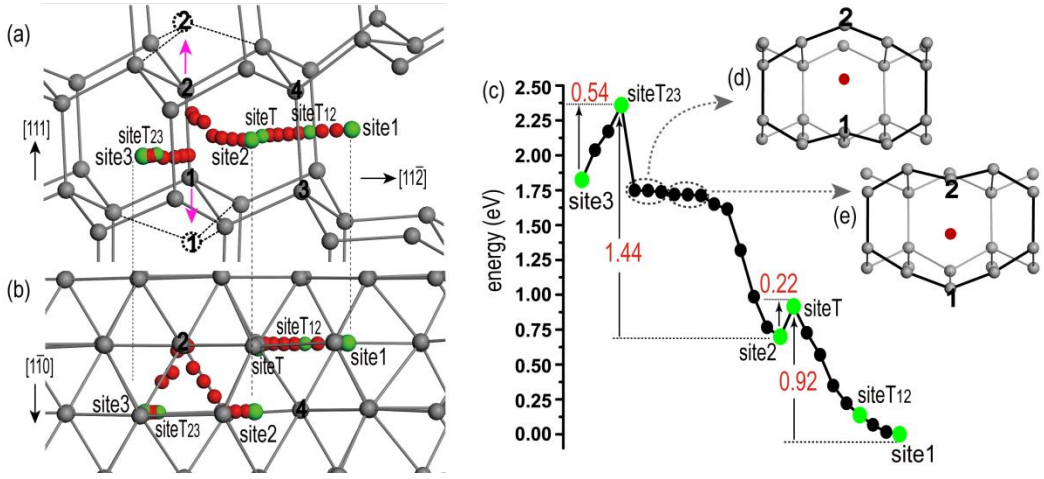

Fig. 4. (a-b) Trajectories of Na and Mg diffusion between sites 3 and 1, and (c) the corresponding migration barriers.

4. Conclusion

In summary, we have shown that cracks may affect the performance of NIBs and MIBs. They may offer more space to host interstitials because of the stress concentration and elongated Si–Si bonds. The increased binding energies indicate that cracks provide more energy favorite sites for Na and Mg than those provided by perfect c-Si. The gradient distribution of the binding energies makes Na and Mg more stable as they get closer to the front of crack. Moreover, the crack tip may raise the negative binding energies of defect-free Si to positive values, enabling it to thermodynamically apply Si anodes in NIBs and MIBs. Further, we studied Na and Mg diffusion between the crack tip and surrounding regions along the loading and crack propagation directions. The stability and migration properties of interstitials are closely related to the atomic structure of the host Si. In these two directions, Na and Mg's thermodynamic/kinetic properties show that they tend to diffuse into the crack tip but not in the opposite directions. In addition, crack facilitates the interstitials to aggregate at the crack tip. Consequently, cracks may imprison interstitials and restrict the charging/discharging rate of NIBs and MIBs.

Acknowledgment

This work was supported by the National Natural Science Foundation of China (Grant Nos. 11102046) and Fundamental Research Funds for the Central Universities.

Reference

[1] J.-M. Tarascon, Key challenges in future Li-battery research, Phil. Trans. R. Soc. A 368 (2010) 3227-3241.

[2] Q. Zhang, J. Mao, W.K. Pang, T. Zheng, V. Sencadas, Y. Chen, Y. Liu, Z. Guo, Boosting the Potassium Storage Performance of Alloy-Based Anode Materials via Electrolyte Salt Chemistry, Adv. Energy Mater. 8 (2018) 1703288.

[3] Y. Yu, Sodium Ion Energy Storage Materials and Devices, Acta Physico-Chimica Sinica, 36 (2020) 1910069.

[4] M. Armand, J.M. Tarascon, Building Better Batteries, Nature 451 (2008) 652-657.

[5] B. Dunn, H. Kamath, J.M. Tarascon, Electrical energy storage for the grid: a battery of choices, Science 334 (2011) 928-935.

[6] G. Harper, R. Sommerville, E. Kendrick, L. Driscoll, P. Slater, R. Stolkin, A. Walton, P. Christensen, O. Heidrich, S. Lambert, A. Abbott, K. Ryder, L. Gaines, P. Anderson, Recycling lithium-ion batteries from electric vehicles, Nature 575 (2019) 75-86.

[7] J.M. Tarascon, Is lithium the new gold? Nat. Chem. 2 (2010) 510.

[8] B.L. Ellis, W.R.M. Makahnouk, Y. Makimura, K. Toghill, L.F. Nazar, A multifunctional 3.5 V iron-based phosphate cathode for rechargeable batteries, Nat. Mater, 6 (2007) 749-753.

[9] D. Saurel, B. Orayech, B. Xiao, D. Carriazo, X. Li, T. Rojo, From Charge Storage Mechanism to Performance: A Roadmap toward High Specific Energy Sodium-Ion Batteries through Carbon Anode Optimization, Adv. Energy Mater. 8 (2018) 1703268.

[10] S.W. Kim, D.H. Seo, X.H. Ma, G. Ceder, K. Kang, Electrode Materials for Rechargeable Sodium-Ion Batteries: Potential Alternatives to Current Lithium-Ion Batteries, Adv. Energy Mater. 2 (2012) 710-721.

[11] H. Wu, Y. Cui, Designing nanostructured Si anodes for high energy lithium ion

batteries, Nano Today 7 (2012) 414-429.

[12] V. Milman, M.C. Payne, V. Heine, R. Needs, J.S. Lin, M.H. Lee, Free energy and entropy of diffusion by ab initio molecular dynamics: Alkali ions in silicon, Phys. Rev. Lett. 70 (1993) 2928-2931.

[13] F. Legrain, O.I. Malyi, S. Manzhos, Comparative computational study of the diffusion of Li, Na and Mg in silicon including the effect of vibrations, Solid State Ionics 253 (2013) 157-163.

[14] C. Yue, Y. Yu, S. Sun, X. He, B. Chen, W. Lin, B. Xu, M. Zheng, S. Wu, J. Li, J. Kang, L. Lin, High Performance 3D Si/Ge Nanorods Array Anode Buffered by TiN/Ti Interlayer for Sodium-Ion Batteries, Adv. Funct. Mater. 25 (2015) 1386-1392.

[15] V.V. Kulish, O.I. Malyi, M.F. Ng, Z. Chen, S. Manzhos, P. Wu, Controlling Na diffusion by rational design of Si-based layered architectures, Phys. Chem. Chem. Phys. 16 (2014) 4260-4267.

[16] F. Legrain, S. Manzhos, Aluminum doping improves the energetics of lithium, sodium, and magnesium storage in silicon: A first-principles study, J. Power Sources 274 (2015) 65-70.

[17] C. Wang, X. Sun, C. Li, G. Wu, B. Wang, Z. Wang, Q. Meng, L. Yang. Effects of defect on the storage and diffusion of Na and Mg interstitials in Si anode, J. Alloys Comp. 654 (2016) 157-162.

[18] O.I. Malyi, T.L. Tan, S. Manzhos, In search of high-performance anode materials for Mg batteries: computational studies of Mg in Ge, Si, and Sn, J. Power Sources 233 (2013) 341-345.

[19] O. Malyi, V.V. Kulish, T.L. Tan, S. Manzhos, A computational study of the insertion of Li, Na, and Mg atoms into Si (111) nanosheets, Nano Energy 2

(2013) 1149-1157.

[20] Y. Kim, Y. Park, A. Choi, N.S. Choi, J. Kim, J. Lee, J.H. Ryu, S.M. Oh, K.T. Lee, An Amorphous Red Phosphorus/Carbon Composite as a Promising Anode Material for Sodium Ion Batteries, Adv. Mater. 25 (2013) 3045-3049.

[21] C. Wang, H. Li, C. Li, G. Wu, T. Sang, L. Yang, Z. Wang, Effects of 30 degrees partial dislocation and stacking fault on Na and Mg storage and diffusion in Si anode, Comp. Mater. Sci. 118 (2016) 16-21.

[22] M.R. Palacin, A. de Guibert, Why do batteries fail? Science 351 (2016) 1253292.

[23] J. Ma, J. Sung, J. Hong, S. Chae, S. Choi, G. Nam, Y. Son, S.Y. Kim, M. Ko, J. Cho, Towards maximized volumetric capacity via pore-coordinated design for large-volume-change lithium-ion battery anodes, Nat. Commun. 10 (2019) 475.

[24] M.T. McDowell, I. Ryu, S.W. Lee, C. Wang, W.D. Nix, Y. Cui, Studying The Kinetics Of Crystalline Silicon Nanoparticle Lithiation With In-Situ Transmission Electron Microscopy, Adv. Mater., 24 (2012) 6034-6041.

[25] T.T. Tran, M.N. Obrovac, Alloy Negative Electrodes for High Energy Density Metal-Ion Cells, J. Electrochem. Soc. 158 (2011) A1411-A1416.

[26] V.L. Chevrier, G.Ceder, Challenges for Na-ion Negative Electrodes, J. Electrochem. Soc. 158(2011) A1011-A1014.

[27] L. Cao, H. Yang, F. Fan, Stress generation during anisotropic lithiation in silicon nanopillar electrodes: A reactive force field study, Phys. Lett. A 383 (2019) 125955.

[28] M.N. Obrovac, L. Christensen, Structural changes in silicon anodes during lithium insertion/extraction, Electrochem. Solid-State Lett. 7 (2004) A93-A96.

[29] F.F. Fan, H. Yang, Z. Zeng, An atomistic perspective on lithiation-induced stress in silicon nanopillars, Scr. Mater. 152 (2018) 74–78.

[30] K. Zhao, G.A. Tritsaris, M. Pharr, W.L. Wang, O. Okeke, Z. Suo, J.J. Vlassak, E. Kaxiras, Reactive flow in silicon electrodes assisted by the insertion of lithium, Nano Lett. 12 (2012) 4397-4403.

[31] M. Mortazavi, J. Deng, V.B. Shenoy, N.V. Medhekar, Elastic softening of alloy negative electrodes for Na-ion batteries, J. Power Sources 225 (2013) 207-214..

[32] C.S. Kang, S.B. Son, J.W. Kim, S.C. Kim, Y.S. Choi, J.Y. Heo, S.S. Suh, Y.U. Kim, Y.Y. Chu, J.S. Cho, S.H. Lee, K.H. Oh, Electrochemically induced and orientation dependent crack propagation in single crystal silicon, J. Power Sources 267 (2014) 739-743.

[33] M.J. Chon, V.A. Sethuraman, A. McCormick, V. Srinivasan, P.R. Guduru, Real-Time Measurement of Stress and Damage Evolution during Initial Lithiation of Crystalline Silicon, Phys. Rev. Lett. 107 (2011) 045503.

[34] Y.S. Choi, M. Pharr, C.S. Kang, S.B. Son, S.C. Kim, K.B. Kim, H. Roh, S.H. Lee, K.H. Oh, J.J. Vlassak, Microstructural evolution induced by micro-cracking during fast lithiation of single-crystalline silicon, J. Power Sources 265 (2014) 160-165.

[35] L. Yang, H.S. Chen, H.Q. Jiang, W.L. Song, D.N. Fang, Lithium redistribution around the crack tip of lithium-ion battery electrodes, Scr. Mater. 167 (2019) 11-15.

[36] C. Wang, C. Zhang, Q. Xue, C. Li, J. Miao, P. Ren, L. Yang, Z. Yang, Atomic mechanism of the distribution and diffusion of lithium in a cracked Si anode, Scr. Mater. 197 (2021) 113807

[37] Y. Liu, G. Lu, Z. Chen, N. Kioussis, An improved QM/MM approach for metals, Modelling Simul. Mater. Sci. Eng. 15 (2007) 275-284.

[38] N. Choly, G. Lu, W. E, E. Kaxiras, Multiscale simulations in simple metals: A

density-functional-based methodology, Phys. Rev. B 71 (2005) 094101.

[39] K. Zhao, G.A. Tritsaris, M. Pharr, W.L. Wang, O. Okeke, Z. Suo, J.J. Vlassak, E. Kaxiras, Reactive flow in silicon electrodes assisted by the insertion of lithium, Nano Lett. 12 (2012) 4397-4403.

[40] J.M. Soler, E. Artacho, J.D. Gale, A. García, J. Junquera, P. Ordejón, D. Sánchez-Portal, The SIESTA method for ab initio order-N materials simulation, J. Phys.: Condens. Matter 14 (2002) 2745.

[41] S. Plimpton, Fast parallel algorithms for short-range molecular dynamics, J. Comput. Phys. 117 (1995) 1-19.

[42] T.-R. Shan, B.D. Devine, T.W. Kemper, S.B. Sinnott, S.R. Phillpot, Charge-optimized many-body potential for the hafnium/hafnium oxide system, Phys. Rev. B 81 (2010) 125328.

[43] J.R. Kermode, T. Albaret, D. Sherman, N. Bernstein, P. Gumbsch, M.C. Payne, G. Csányi, A. De Vita, Low-speed fracture instabilities in a brittle crystal, Nature 455 (2008) 1224-1227.

[44] J.P. Perdew, K. Burke, M. Ernzerhof, Generalized gradient approximation made simple, Phys. Rev. Lett. 77 (1996) 3865-3868.

[45] M. Kaukonen, J. Peräjoki and R.M. Nieminen, G. Jungnickel and Th. Frauenheim, Locally activated Monte Carlo method for long-time-scale simulations, Phys. Rev. B 61 (2000) 980-987.

Figure1

Click here to access/download;Figure;Fig.1 binding energy400-01.tif

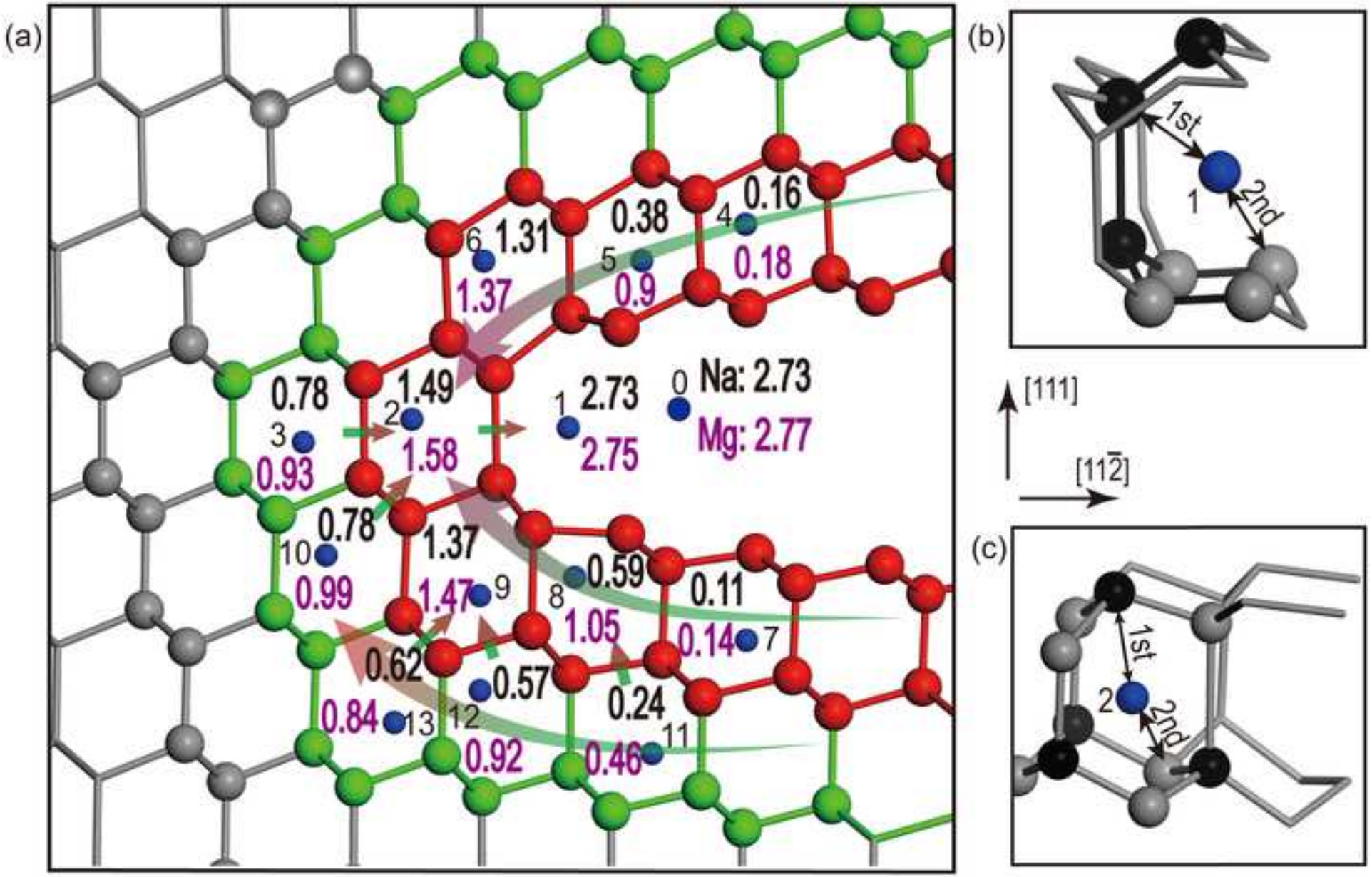

Figure2

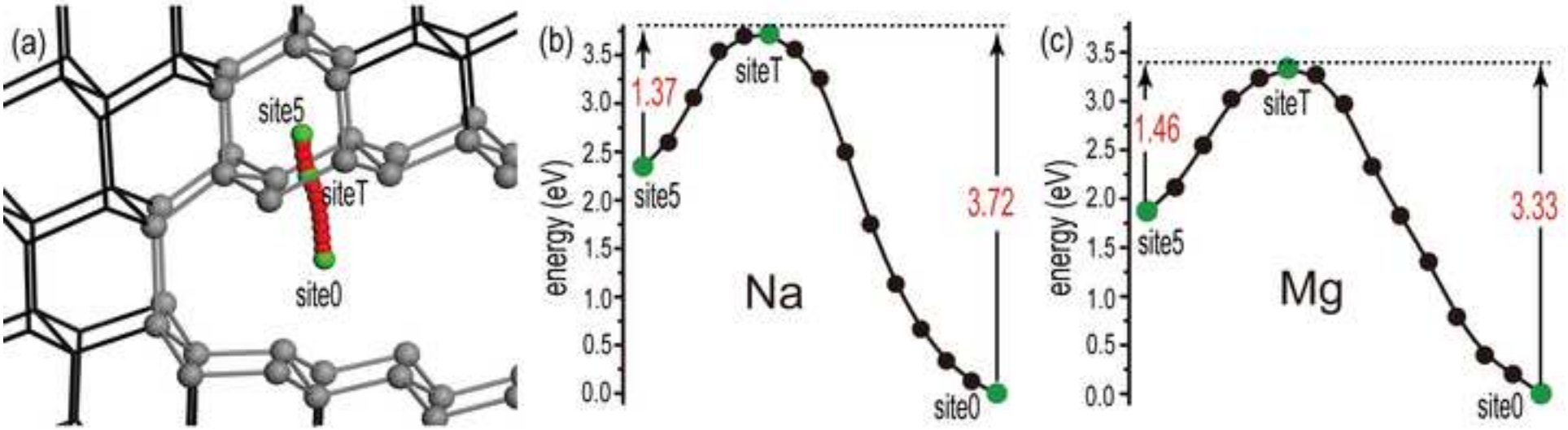

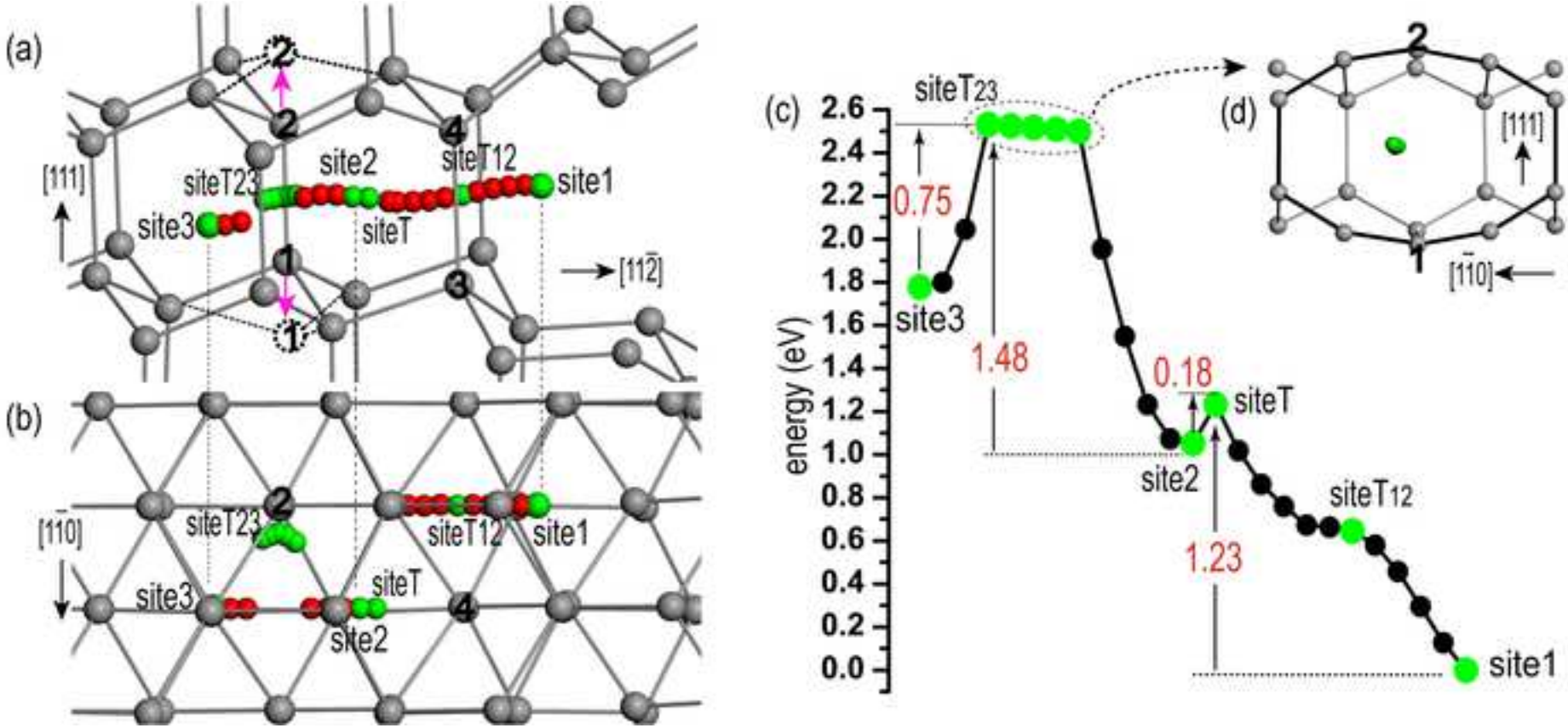

Figure4

Click here to access/download;Figure;Fig4.Mg0-2-500-01.tif